Macromolecules
ARTICLE

Macromolecules **2010**, *43*, 7583–7593 **7583**
DOI: 10.1021/ma101066p

Molecular Structure Dependence of Out-of-Plane Thermal Diffusivities in Polyimide Films: A Key Parameter for Estimating Thermal Conductivity of Polymers

Daisuke Yorifuji and Shinji Ando*

Department of Chemistry and Materials Science, Tokyo institute of Technology, Ookayama 2-12-1-E4-5, Meguro-ku, Tokyo 152-8552, Japan

Received May 13, 2010; Revised Manuscript Received July 21, 2010

ABSTRACT: The dependence of thermal diffusivity along the out-of-plane direction ($D_\perp$) on molecular structure, chain orientation, and molecular packing was extensively investigated for 21 kinds of aromatic and semiaromatic polyimide (PI) films using temperature wave analysis. The inherent structural character and the orientaion of polymer chains were quantitatively evaluated based on the polarizability anisotropy calculated for the repeating units of PIs using the density functional theory (DFT) and the observed in-plane/out-of-plane birefringences (Δn). Following the findings, a new parameter, $\Phi_\perp$, which can be used to estimate the $D_\perp$ of PIs, is proposed based on modified Lorentz−Lorenz and Vuks equations, and the validity of the parameter was evaluated. The $\Phi_\perp$ is readily estimated from the experimental values of in-plane ($n_{||}$) and out-of-plane ($n_\perp$) refractive indices and the Δn of PI films. The positive and linear correlation between $D_\perp$ and $\Phi_\perp$ revealed that not only an increase in the degree of molecular orientations along the out-of-plane direction, but also a densification of molecular packing is effective for an enhancement of $D_\perp$.

Introduction

Recently, the microelectronics and optoelectronics industries have begun to pay more attention to the potential of thermally stable polymers, such as epoxy resins, polysiloxanes, polyimides, and polybenzoxazoles, as promising low-dielectric insulator films or passive/active layers for photonic devices.[1,2] With this technological trend, there is growing interest in the properties of such high-performance polymers. The thermal conductivity of polymers is of particular interest and importance because it governs the temporal thermal behavior of polymer-containing products. In particular, the enhancement and control of the thermal conductivity of polymer films are of great significance for the applications of electronic insulators. However, owing to their disordered structures, the much lower thermal conductivity of polymers compared with those of metals and ceramics causes significant disadvantages in overheating and lifetime reduction in electronic devices and components. Hence, there has been a strong demand for the enhancement and precise control of the thermal conductivity of polymers.

In a semicrystalline polymer, significant anisotropy in thermal conductivity can be observed when the polymer main chains are oriented along a certain direction.[3,4] This can be explained in terms of "phonon focusing".[5] Atomic vibrations, which transfer thermal energy, are effectively transmitted along the polymer main chains connected by covalent bonds ("intrachain thermal transfer"). In contrast, atomic vibrations are not effectively transmitted among polymer chains ("interchain thermal transfer"), in which interchain interactions such as van der Waals and dipolar−dipolar interactions are much weaker than covalent bonds. Choy and co-workers have shown that the thermal conductivity of highly oriented polyethylene ($\lambda_{||}$) at 300 K is 13.8 W/mK along the stretching direction (draw ratio: 25), whereas the value perpendicular to the stretching direction ($\lambda_\perp$) is only 0.235 W/mK.[6] In amorphous polymers which possess neither ordered nor oriented structures, the thermal conductivity and its anisotropy are much smaller than those of semicrystalline polymers due to the significant scattering of phonons by structural inhomogeneities. Thereby, the mean free path of phonons is reduced to the order of a few angstroms. In the amorphous polymers, nevertheless, the thermal conductivity becomes anisotropic ($\lambda_{||} > \lambda_\perp$) when the polymer main chains are oriented along a certain direction. Since the covalent bonds along the chains are much stronger than van der Waals and dipolar−dipolar interactions, the average phonon velocity in the oriented direction should be larger than those along the other directions due to the difference of the force constants of the molecular interaction.[3,7]

The thermal conductivity λ (W/mK) of matter can be written as:[7]

$$\lambda = \rho C_p D \quad (1)$$

where ρ is the density (kg/m^3), C_p the heat capacity at constant pressure (J/kg·K), and D the thermal diffusivity (m^2/s). The thermal diffusivity (D) is proportional to the product of average phonon velocity (v (m/s)) and mean free path of phonons (l (m)). For noncrystalline polymers and soft materials, the values of ρC_p vary only marginally at room temperature, thus D is the most prominent factor for their thermal conductivity. For instance, Venerus and co-workers measured thermal diffusivity in cross-linked amorphous polymers subjected to uniaxial elongational deformation. They reported the thermal diffusivities parallel ($D_{||}$) and perpendicular ($D_\perp$) to the stretch direction were linearly increased and decreased with stretch ratio, respectively.[8,9]

Polyimides (PIs) have been widely used in electric, microelectronic and photonic applications, such as electrical insulators and substrates for flexible printed circuit boards and optical waveguides, due to their high thermal stability, good mechanical

*Corresponding author. E-mail: sando@polymer.titech.ac.jp. Telephone: +81-3-5734-2137. Fax: +81-3-5734-2889..

Published on Web 08/16/2010

properties, and favorable electrical properties.[10] PI films which have been used in microelectronics are, in general, prepared by spin coating of a precursor solution of PI, poly(amic acid) (PAA), or PI solutions followed by thermal curing at elevated temperatures. The spin-coating process causes orientation of PAA or PI chains to be along the in-plane direction of the substrate, which is called in-plane orientation, due to the centrifugal force during spinning. In addition, the volume shrinkage of the PI films during drying and curing also causes preferential alignment of polymer chains in the film plane. A few researches have reported the anisotropic thermal conductivities and/or diffusivities of PI films parallel and perpendicular to the film plane.[11,12] Kurabayashi and co-workers have reported that the thermal diffusivity of PI (Du Pont PI 2556) along the in-plane direction ($D_{||}$) is 4−8 times larger than that along the out-of-plane direction ($D_{\perp}$).[11] They also explained that the anisotropy originates from the in-plane orientation of polymer chains. Morikawa and co-workers reported the dependence of $D_{||}$ and $D_{\perp}$ on the molecular structure and the main chain orientation of PIs for several PI films.[13] Although appreciable differences were observed in $D_{||}$, little structure and orientation dependences were detected in $D_{\perp}$. The degree of main chain orientation in PI films, however, depends on the chemical structure of PIs,[14] and the in-plane/out-of-plane orientation of PI chains should influence not only the anisotropy in thermal diffusivity ($D_{||} - D_{\perp}$) but also $D_{\perp}$ itself. Moreover, the $D_{\perp}$ in polymer films, has a dominant influence on heat transfer in microelectronic applications such as multilayer insulators.

The purpose of this study is to investigate the dependence of $D_{\perp}$ on the molecular structures, orientation of PI chains, and degree of molecular packing for spin-coated and thermally cured aromatic and semiaromatic PI films. The relationships among the parameters which represent the structural characteristics and the properties of PIs were extensively investigated for 21 kinds of PIs having different structures. The $D_{\perp}$ values of PI films were measured by temperature wave analysis (TWA), which estimates the thermal diffusivity of thin films from the frequency-dependent phase shifts of temperature waves transmitted along the out-of-plane direction.[13,15] The molecular structure and orientation of PI chains in the films were evaluated by 1) the degree of chain orientation, estimated by in-plane/out-of-plane birefringence (Δn), 2) the rigidity/linearity of polymer repeating units, estimated by the electric dipole polarizability anisotropy ($\Delta\alpha/V_{vdw}$),[16] and 3) the degree of molecular packing represented by the packing coefficients (K_p). We propose a new parameter, $\Phi_{\perp}$, based on modified Lorentz−Lorenz and Vuks equations. This parameter can be readily deduced from experimental in-plane ($n_{||}$) and out-of-plane ($n_{\perp}$) refractive indices, and used as a measure for $D_{\perp}$ of PI films. By relating $D_{\perp}$ to the molecular structure of PIs, the validity of the parameter was extensively examined.

Theoretical Basis

Evaluation of Molecular Chain Orientation through Birefringence. The degree of polymer chain orientation is directly related to the anisotropy in the optical, dielectrical, and mechanical properties of polymers, and it has been widely studied by using anisotropic parameters such as optical birefringence,[17] dichroism in polarized FT-IR spectroscopy,[18] and dichroic ratios in UV−visible absorption spectra using doped dyes.[19] In particular, birefringence has been widely used for concise estimation of chain orientation because of its robustness and high degree of accuracy.

In-plane/out-of-plane birefringence (Δn) is the anisotropy expressed by the refractive index difference defined as:

$$\Delta n = n_{||} - n_{\perp} \tag{2}$$

where $n_{||}$ and $n_{\perp}$ are the refractive indices parallel and perpendicular to the film plane, respectively. These are sometimes denoted as n_{TE} (refractive index of transverse electric wave) and n_{TM} (refractive index of transverse magnetic wave), respectively. Since the orientations of polymer chains are isotropic in the film plane for spin-coated films, the average refractive index (n_{av}) is approximated as:

$$n_{av} = \frac{2n_{||} + n_{\perp}}{3} \tag{3}$$

In a rotationally symmetrical system of films, the value of Δn is directly related to the degree of chain orientation with respect to the symmetrical axis:

$$\Delta n = P_{200}\,\Delta n^0 = \frac{1}{2}(3\langle\cos^2\Theta\rangle - 1)\Delta n^0 \tag{4}$$

$$\Delta n^0 = n_{||}{}^0 - n_{\perp}{}^0 \tag{5}$$

where Δn^0 is the intrinsic birefringence, P_{200} the second-order orientation coefficient, and Θ the polar angle between the principal axis of the main chain and the symmetrical axis.[18,20] $n_{||}{}^0$ and $n_{\perp}{}^0$ are respectively the refractive indices parallel and perpendicular to the chain direction in an idealized system with complete orientation of the main chain. When n_{av} is unchanged by orientation in a certain direction, eq 3 can be rewritten as

$$n_{av} = \frac{2n_{||} + n_{\perp}}{3} = \frac{2n_{||}^0 + n_{\perp}^0}{3} \tag{6}$$

In this study, the experimental values of $n_{||}$ and $n_{\perp}$ were precisely measured using the prism-coupling method.

Relationships among Refractive Index, Polarizability, and Molecular Packing. The relationship between the average refractive index (n_{av}) and the average polarizability (α_{av}) is represented by the Lorentz−Lorenz equation:[21,22]

$$\frac{n_{av}{}^2 - 1}{n_{av}{}^2 + 2} = \frac{4\pi}{3}\frac{\alpha_{av}}{V_{int}} = \frac{4\pi}{3}\frac{\rho N_A}{M}\alpha_{av} \tag{7}$$

Here V_{int} is the intrinsic volume of the repeating unit, ρ the density, M the molecular weight, N_A the Avogadro number, and α_{av} the average molecular polarizability, in which the electric dipole polarizability is a second-rank Cartesian tensor, represented by $\hat{\alpha}$. The degree of polymer chain packing is represented as the molecular packing coefficient (K_p), which is defined as

$$K_p = \frac{V_{vdw}}{V_{int}} \tag{8}$$

where V_{vdw} is the van der Waals volume of the repeating unit and V_{int} the summation of V_{vdw} and intermolecular free volume; for instance, loose chain packing leads to a small K_p. Thereby, eq 7 can then be rewritten as

$$\Phi_{av} \equiv \frac{n_{av}{}^2 - 1}{n_{av}{}^2 + 2} = \frac{4\pi}{3}K_p\frac{\alpha_{av}}{V_{vdw}} \tag{9}$$

Since the left-hand term of eq 9 monotonously increases with an increase in n_{av}, small values of α_{av} and K_p lead to a small n_{av}. In this study, the K_p values of PI films were precisely estimated from the experimental n_{av} and the calculated α_{av}/V_{vdw} values based on eq 9.

In an idealized system with complete chain orientation, the molecular polarizability anisotropy of the polymer repeating

Scheme 1. (a) Molecular Structures of Polyimides (PIs) and (b) Model Structures for Computation of Polarizability Tensors of the Corresponding PIs

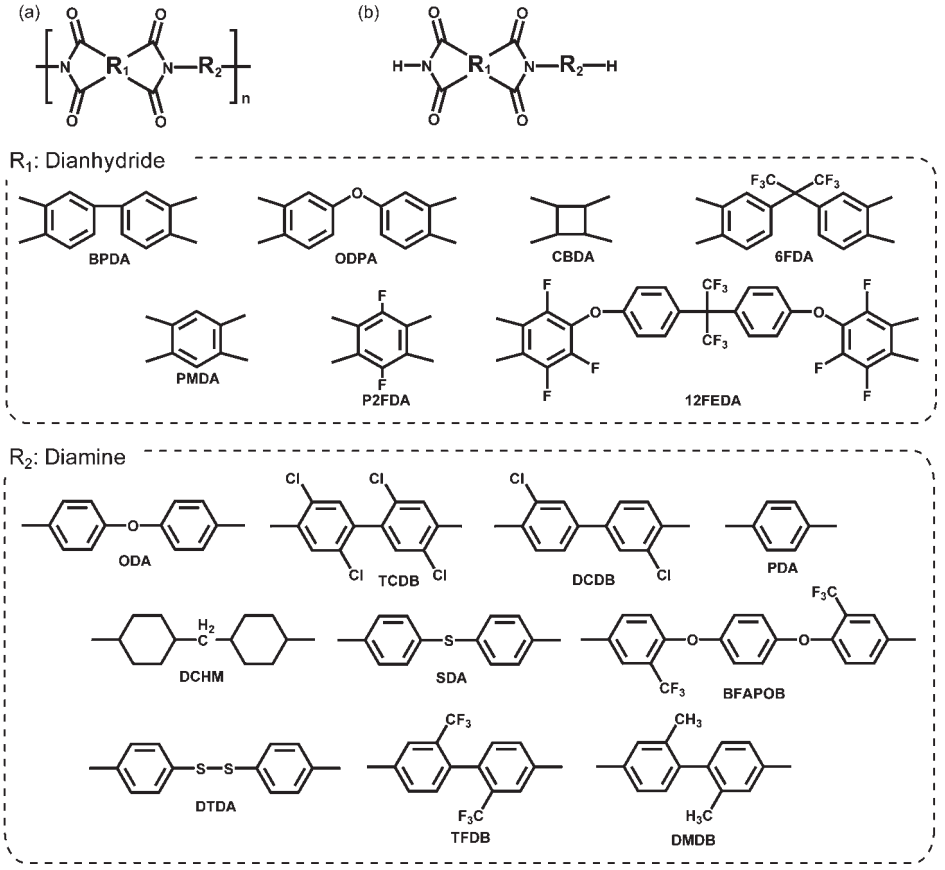

unit should be directly related to the anisotropic refractive indices. Hence, both $n_{||}{}^0$ and $n_{\perp}{}^0$ are estimated using the Vuks equations[23] as follows:

$$\frac{(n_{||}^0)^2-1}{n_{\mathrm{av}}{}^2+2}=\frac{4\pi}{3}\frac{\alpha_{||}}{V_{\mathrm{int}}}=\frac{4\pi}{3}K_{\mathrm{p}}\frac{\alpha_{||}}{V_{\mathrm{vdw}}} \tag{10}$$

$$\frac{(n_{\perp}^0)^2-1}{n_{\mathrm{av}}{}^2+2}=\frac{4\pi}{3}\frac{\alpha_{\perp}}{V_{\mathrm{int}}}=\frac{4\pi}{3}K_{\mathrm{p}}\frac{\alpha_{\perp}}{V_{\mathrm{vdw}}} \tag{11}$$

where $\alpha_{||}$ and $\alpha_{\perp}$ are the polarizability components parallel and perpendicular to the main chain direction.

Rigidity/Linearity of Polymer Repeating Units Estimated by the Polarizability Anisotropy. For a spin-coated film of a polymer containing plural aromatic rings, the polarizability along the main chain can be much larger than that perpendicular to the main chain ($\alpha_{||} > \alpha_{\perp}$). When the main chains are preferentially oriented in the film plane, this results in a larger $n_{||}$ than $n_{\perp}$ with a positive Δn. This is the case for almost all PI films. The molecular axis system (o-*XYZ*) for the polarizability tensors ($\hat{\alpha}$) of the PI repeating unit is defined as follows: the *Z*-axis is parallel to the PI main chain, the *Y*-axis is perpendicular to the imide plane, and the *X*-axis is parallel to the direction which links two imide-carbonyl carbons. Then, the polarizability anisotropy ($\Delta\alpha$) is defined as

$$\Delta\alpha = \alpha_{zz}-\frac{\alpha_{xx}+\alpha_{yy}}{2} \tag{12}$$

where α_{zz}, α_{yy}, and α_{xx} are the principal values of the average polarizability tensor along the *Z*-, *Y*-, and *X*-axes, respectively. In addition, the average polarizability (α_{av}) is defined as:

$$\alpha_{\mathrm{av}} = \frac{\alpha_{xx}+\alpha_{yy}+\alpha_{zz}}{3} \tag{13}$$

Assuming that the polarizability tensor of a polymer chain can be expressed as a uniaxial ellipsoid with rotational symmetry, $\alpha_{||}$ and $\alpha_{\perp}$ can be defined as

$$\alpha_{||} = \alpha_{zz} \tag{14}$$

$$\alpha_{\perp} = \frac{\alpha_{xx}+\alpha_{yy}}{2} \tag{15}$$

In this study, the rigidity/linearity of polymer repeating units is represented by the $\Delta\alpha$ value, calculated using density functional theory (DFT).

Experimental Section

Materials. Twenty-one kinds of PIs with different molecular structures used in this study were prepared from seven dianhydrides and 10 diamines (see Scheme 1a). The commercial sources and the purification conditions for the dianhydrides (R_1 in Scheme 1) and the diamines (R_2 in Scheme 1) are listed in Tables 1 and 2, respectively. The dianhydrides of CBDA, 6FDA, P2FDA, and 12FEDA, and the diamines of TCDB, DCDB, TFDB, and DMDB were kindly supplied by the companies listed in the Tables and the other source materials were purchased from the listed companies. All the companies are located in Japan. BFAPOB was synthesized according to the literature.[24] The diamines, except for TFDB and BFAPOB, were purified by recrystallization followed by sublimation under reduced pressure.

Table 1. Commercial Sources and Purification Conditions of Dianhydrides

dianhydride	source	conditions of purification
3,3′;4,4′-biphenyltetracarboxylic dianhydride (BPDA)	Wako Pure Chemicals Industries, Ltd.	dried at 180 °C under reduced pressure
3,3′;4,4′-diphenylethyl ether tetra-carboxylic dianhydride (ODPA)	Tokyo Chemical Industry Co., Ltd.	purified by sublimation under reduced pressure
1,2;3,4-cyclobutanetetracarboxylic dianhydride (CBDA)	JSR corporation	dried at 120 °C under reduced pressure
4,4′-(hexafluoroisopropylidene) diphthalic dianhydride (6FDA)	AZ Electronic Materials (Japan) K.K.	purified by sublimation under reduced pressure
1,2;4,5-benzenetetracarboxylic dianhydride (PMDA)	Kanto Kagaku Co., Ltd.	purified by sublimation under reduced pressure
3,6-difluoro-1,2;4,5-benzenetetra-carboxylic dianhydride (P2FDA)	NTT Advanced Technology Co., Ltd.	used as received
[4-(2,5,6-trifluoro-3,4-dicarboxyphenoxy)phenyl]-1,1,1,3,3,3-hexafluoropropane dianhydride (12FEDA)	Nippon Shokubai Co.ss, Ltd.	used as received

Table 2. Commercial Sources and Purification Conditions of Diamines

diamine	source	conditions of purification
4,4′-diaminodiphenyl ether (ODA)	Kanto Kagaku Co., Ltd.	recrystallization from tetrahydrofuran
2,2′;5,5′-tetrachlorobenzidine (TCDB)	Wakayama Seika Co. Ltd.	purified by sublimation
3,3′-dichlorobiphenyl-4,4′-diamine (DCDB)	Fuji Film Co. Ltd.	purified by sublimation
p-phenylenediamine (PDA)	Kanto Kagaku Co., Ltd.	recrystallization from tetrahydrofuran
4,4′-diaminodicyclohexylmethane (DCHM)	Tokyo Chemical Industry Co., Ltd.	recrystallization from hexane
4,4′-thiodianiline (SDA)	Wako Pure Chemicals Industries, Ltd.	purified by sublimation
1,4-bis(4-amino-2-trifluoro-methylphenoxy)benzene (BFAPOB)		synthesized according to ref 24
4,4′-dithiodianiline (DTDA)	Tokyo Chemical Industry Co., Ltd.	recrystallization from methanol
2,2-bis(trifluoro-methyl)-4,4′-diaminobiphenyl (TFDB)	Central Glass Co., Ltd.	used as received
2,2′-dimethyl-4,4′-diamino-biphenyl (DMDB)	Wakayama Seika Co. Ltd.	recrystallization from tetrahydrofuran

The precursor solutions of aromatic PIs, poly(amic acid)s (PAAs), were prepared by addition polymerization of equimolar amounts of dianhydrides and diamines. A dried powdery dianhydride was added to an *N*,*N*-dimethylacetamide (DMAc, purchased from Aldrich, anhydride grade) solution of a diamine and stirred at room temperature for 24 h. All procedures were carried out in a nitrogen-purged glovebox. The precursor of semialiphatic BPDA-DCHM was prepared by the *in situ* silylation method[25,26] to avoid salt formation between unreacted amino groups and the carboxyl groups of the dianhydride moiety. Bis(trimethylsilyl)trifluoroacetamide (99+%, purchased from Aldrich) was used as a silylating agent for the method. PI films were prepared by thermal imidization of PAA solutions spin-coated onto 4-in. fused silica substrates, followed by soft-baking at 70 °C for 1 h and subsequent thermal curing by a one-step imidization procedure: the final curing conditions were 350 °C for 1.5 h for aromatic PIs and 300 °C for 1.5 h for semiaromatic PIs (CBDA-ODA and BPDA-DCHM). The heating rate was 4.6 °C/min from 70 to 350 °C and 300 °C, respectively. All curing procedures were conducted under nitrogen flow (2 *l*/min). All PI films thus prepared had very smooth surfaces with thicknesses of 15−39 μm.

Thermal Diffusivity Measurement. The thermal diffusivities along the out-of-plane direction ($D_\perp$) of 21 different kinds of PI films were measured with an AC temperature wave analyzer (ai-Phase mobile 1, ai-Phase Co. Ltd.) based on the TWA method at room temperature. The details of TWA method have been reported in reference.[13,15] In the TWA technique, an AC temperature wave generated from the heater in direct contact with one side of the film passes through the film in the thickness (out-of-plane) direction. The phase delay of the wave was detected by the sensor placed on the other side of the film. $D_\perp$ was directly estimated from the phase delay when the angular frequency of the temperature wave and the film thickness were known. Thicknesses of PI films were measured by the thickness meter equipped with the TWA analyzer. Each film was measured three times, which guarantees error ranges of ±5% in $D_\perp$ and ±3% in film thickness, and the average value was adopted as a measured value.

Refractive Index Measurement. The in-plane ($n_{||}$) and out-of-plane ($n_\perp$) refractive indices of PI films formed on fused silica substrates were measured using a prism coupler (Metricon, PC-2010) at a wavelength of 1.32 μm. The average refractive indices (n_{av}) were calculated using eq 3. The anisotropy in the refractive index, that is, the in-plane/out-of-plane birefringence (Δn), was calculated using eq 2.

Polarizability Tensor Calculations. The density functional theory (DFT) with a three-parameter Becke-style hybrid functional (B3LYP) was used for the calculation of the molecular polarizability of PI repeating unit.[27−29] All the calculations were performed with a Gaussian-03 E.01 program package[30] installed in the Global Scientific Information and Computing Center (GSIC), Tokyo Institute of Technology. The geometry optimization of the PI model structures depicted in Scheme 1b was carried out using the 6-311G(d) basis set. The polarizability tensors were calculated by using the 6-311++G(d,p) basis set followed by rotating around the molecular axis frame (o-*XYZ*). We previously reported that the polarizability tensors of polymers can be quantitatively reproduced by using this basis set.[14] For the PI models containing BPDA, ODPA, 6FDA and 12FEDA dianhydride moieties, the *Y*-axis is taken as the average of the vectors perpendicular to the two imide planes. The polarizability anisotropies ($\Delta\alpha$) and average polarizabilities (α_{av}) were calculated using eqs 12 and 13, respectively. The van der Waals volumes (V_{vdw}) of the PI models were calculated on the basis of Slonimski's method using the molecular geometry optimized using the 6-311G(d) basis set,[31] in which the van der Waals radii of atoms reported by Bondi were used.[32] The orientation coefficient P_{200} was determined using the experimental Δn and the calculated Δn^0 values in eqs 4 and 5, in which the $n_{||}{}^0$ and $n_\perp{}^0$ values were estimated from eqs 10 and 11.

Results and Discussion

Molecular Structure and Orientation Dependences of Out-of-Plane Thermal Diffusivity. The out-of-plane thermal diffusivities ($D_\perp$), refractive indices and birefringences ($n_{||}$, $n_\perp$, n_{av}, Δn), and film thicknesses of the PI films prepared in this study are listed in Table 3. Among the PIs, a fully aromatic PI of BPDA-ODA showed the highest $D_\perp$ value (18.3×10^{-8} m^2/s) and a highly fluorinated PI of P2FDA-TFDB showed the lowest $D_\perp$ value (8.8×10^{-8} m^2/s). In addition, the PIs derived from BPDA and ODPA dianhydrides (R_1 in Scheme 1) and

Table 3. Out-of-Plane Thermal Diffusivities ($D_\perp$), In-Plane Refractive Indices ($n_{||}$), Out-of-Plane Refractive Indices ($n_\perp$), Average Refractive Indices (n_{av}), In-Plane/Out-of-Plane Birefringences (Δn), and Thicknesses of Polyimide Films

dianhydride	diamine	thermal diffusivity $D_\perp(\times 10^{-8}$ m^2/s)	$n_{||}$	$n_\perp$	n_{av}	Δn	thickness (μm)
BPDA	ODA	18.3	1.6941	1.6659	1.6847	0.0282	26.2
	TCDB	18.1	1.6745	1.6497	1.6662	0.0248	38.8
	DCDB	18.0	1.7169	1.6553	1.6963	0.0616	38.7
	PDA	16.5	1.7731	1.6448	1.7303	0.1283	25.8
	DCHM	16.2	1.6133	1.6038	1.6102	0.0095	21.4
	SDA	13.8	1.6980	1.6784	1.6915	0.0196	18.1
	BFAPOB	13.6	1.5964	1.5902	1.5943	0.0062	19.9
	DTDA	13.0	1.7109	1.7028	1.7082	0.0081	19.9
	TFDB	12.3	1.6105	1.5648	1.5953	0.0457	23.9
	DMDB	10.3	1.7210	1.5867	1.6762	0.1343	15.6
ODPA	ODA	17.6	1.6511	1.6413	1.6478	0.0098	27.8
	SDA	13.3	1.6718	1.6709	1.6715	0.0009	32.9
	BFAPOB	12.8	1.5838	1.5767	1.5814	0.0071	30.7
CBDA	ODA	13.0	1.6025	1.5765	1.5938	0.0259	19.7
6FDA	ODA	12.3	1.5671	1.5573	1.5638	0.0097	21.7
PMDA	DTDA	12.0	1.7214	1.6892	1.7107	0.0321	15.7
	ODA	11.5	1.7097	1.5962	1.6719	0.1135	26.3
P2FDA	ODA	11.3	1.6661	1.5885	1.6402	0.0776	24.8
	TCDB	9.9	1.6582	1.5784	1.6316	0.0797	28.2
	TFDB	8.8	1.5935	1.5133	1.5667	0.0802	22.8
12FEDA	DCHM	8.9	1.5144	1.5103	1.5130	0.0041	38.6

those derived from ODA diamine (R_2 in Scheme 1) exhibited higher $D_\perp$ values than those from the other source materials. In contrast, the PIs derived from fluorinated dianhydrides (6FDA and 12FDEA), fluorinated diamines (TFDB and BFAPOB), and sulfur-containing diamines (SDA and DTDA) exhibited lower $D_\perp$ values. Moreover, the PIs derived from the dianhydrides which include only one benzene ring (PMDA and P2FDA) and one alicyclic ring (CBDA) exhibited relatively low $D_\perp$ values. These facts suggest that the PIs consisting of sequential aromatic structures, such as the biphenyl moiety, as well as a bent linkage (ether or thioether) without bulky side chains ($-CH_3$ and $-CF_3$) and heavy sulfur atoms demonstrate relatively high $D_\perp$ values.

Kurabayashi and co-workers modeled the impact of molecular orientation in spin-coated polymer films on their anisotropy in thermal conductivity using the experimental Δn, and they reported that a random molecular structure could increase the out-of-plane thermal conductivity due to the low degree of orientation along the in-plane direction.[11] Following their prediction, the relationship between the experimental $D_\perp$ and Δn values was investigated for the PI films prepared in this study (see Table 3 and Figure 1a). For the PIs derived from BPDA dianhydride (indicated by filled circles), the Δn decreases in the order of the diamine moiety: DMDB > PDA > DCDB > TFDB > ODA > TCDB > SDA > DCHM > DTDA > BFAPOB. As expected from the structures, the rigid rod diamines (DMDB, PDA, DCDB, and TFDB) exhibited large values of Δn (> 0.0457), whereas the aromatic diamines having bent and rotatable linkages (ODA, SDA, DTDA, and BFAPOB) and the alicyclic diamine (DCHM) exhibited smaller Δn values (< 0.0282). In particular, BPDA-DCHM, BPDA-DTDA, and BPDA-BFAPOB showed very small Δn values (< 0.0095). On the other hand, for the PIs derived from ODA diamine, the Δn values decrease in the order of the dianhydride moiety: PMDA > P2FDA > BPDA > CBDA > ODPA > 6FDA. This order is also related to the rigidity/linearity of the dianhydride structure. The aromatic dianhydrides having bent and rotatable linkages (ODPA and 6FDA) exhibited smaller Δn values. The scattered plots in Figure 1a indicate that the $D_\perp$ of PI films could not be solely controlled by the degree of molecular orientation, as reflected by Δn. For example, 12FEDA-DCHM is a PI with low orientation along the in-plane direction and exhibits a small Δn value, but its $D_\perp$ is very small. The plots of $D_\perp$ against orientation coefficient P_{200} also exhibited a similar tendency (see Figure S1a in the Supporting Information). This is because the variations in intrinsic birefringence (Δn^0) among the examined PIs are not so large.

For the estimation of Δn^0 of PIs, we previously reported that rigid and linear structures of repeating units accompany a large polarizability anisotropy per volume ($\Delta\alpha/V_{vdw}$).[14] Since the "intrachain thermal transfer" within the polymer chains is faster and more efficient than the "interchain thermal transfer" among the polymer chains, the rigidity/linearity of the polymer repeating unit is a key factor in determining the anisotropy in thermal diffusivity. Thus, the relationship between $D_\perp$ and $\Delta\alpha/V_{vdw}$ was investigated. Table 4 lists the calculated values of van der Waals volumes (V_{vdw}), principal components of the polarizability tensor (α_{xx}, α_{yy}, and α_{zz}), average polarizability perpendicular to the PI main chain ($(\alpha_{xx} + \alpha_{yy})/2$), average polarizability per volume (α_{av}/V_{vdw}), and $\Delta\alpha/V_{vdw}$. The calculated values of α_{xx}, α_{yy}, and α_{zz} were obtained by rotating the polarizability tensor of a model structure of repeating units in the molecular frame, in which the α_{ZZ} axis corresponds to the longest molecular axis. Since molecular polarizability has the same dimension as molecular volume, the absolute values of α_{av} and $\Delta\alpha$ were divided by V_{vdw} for mutual comparison. Figure 1b shows the relationship between $D_\perp$ and $\Delta\alpha/V_{vdw}$ for the PIs examined. The positive and weakly correlated relation may suggest that the rigidity/linearity of PI repeating units could affect their $D_\perp$. In addition, the PIs derived from BPDA (BPDA-R_2) exhibit larger $D_\perp$ and $\Delta\alpha/V_{vdw}$ values than those of the PIs from other dianhydrides (other R_1-R_2). The large $\Delta\alpha/V_{vdw}$ values for the PIs from BPDA are attributable to the following two factors. One is the fraction of imide rings in the repeating units.[14] The imide carbonyl (C=O) enhances the polarizability perpendicular to the main chain because the $\Delta\alpha/V_{vdw}$ values decrease as the fraction of imide rings increases. Hence, the PIs derived from BPDA, ODPA, 6FDA, and 12FEDA with relatively low imide fractions exhibited larger $\Delta\alpha/V_{vdw}$ values than those from PMDA, CBDA, and P2FDA with higher imide fractions. The other factor is the rigidity/linearity of the dianhydride moiety. Since the bent and rotatable linkages between

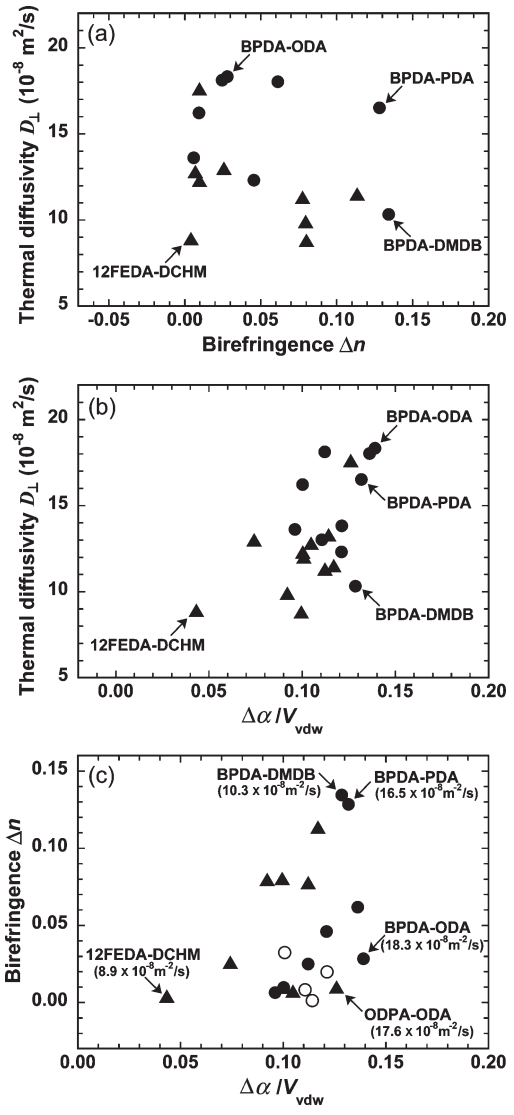

Figure 1. Relationships among the out-of-plane thermal diffusivity ($D_\perp$), in-plane/out-of-plane birefringence (Δn), and polarizability anisotropy per unit volume ($\Delta\alpha/V_{vdw}$) of PI films. (a) $D_\perp$ versus Δn, (b) $D_\perp$ versus $\Delta\alpha/V_{vdw}$, and (c) Δn versus $\Delta\alpha/V_{vdw}$ for the PIs derived from (●) BPDA dianhydride, (▲) other dianhydrides, and (○) diamines containing sulfur atoms (sulfur-containing PIs).

two aromatic rings, such as −O− and −C(CF$_3$)$_2$−, in ODPA, 6FDA, and 12FEDA dianhydrides significantly reduce the rigidity/linearity of the repeating units, the $\Delta\alpha/V_{vdw}$ values also decrease as the fraction of bent structures increases. Hence, the PIs derived from BPDA exhibited larger $\Delta\alpha/V_{vdw}$ values than those from the other dianhydrides. On the other hand, among the PIs derived from BPDA, the $\Delta\alpha/V_{vdw}$ values decreased in the order of the diamine moiety: ODA > PDA > DCDB > DMDB > TFDB > SDA > TCDB > DTDA > DCHM > BFAPOB. This order differs from that of the $D_\perp$ values, which indicates that the $D_\perp$ of PIs could not be controlled solely by the rigidity/linearity of the repeating unit structure. For instance, BPDA-DMDB exhibits a large $\Delta\alpha/V_{vdw}$ value but its $D_\perp$ value is the smallest of the PIs derived from BPDA.

A structural parameter which governs $D_\perp$, thus far, could not be deduced only from the degree of polymer chain orientation or the rigidity/linearity of the molecular structure. Thereby, to combine these effects on $D_\perp$, the relationship between Δn and $\Delta\alpha/V_{vdw}$ is depicted in Figure 1c. It should be noted that, when the plots are compared with the $D_\perp$ in Table 1, PI films having small Δn and large $\Delta\alpha/V_{vdw}$ values tend to exhibit high $D_\perp$ values. The relationship between P_{200} and $\Delta\alpha/V_{vdw}$ also exhibits the same tendency (see Figure S1b in Supporting Information). Scheme 2 shows the optimized molecular structures of the repeating units and the schematic illustrations of the ellipsoids of the molecular polarizabitlity tensor for three representative PIs with characteristic features: (a) BPDA-ODA with a small Δn and a large $\Delta\alpha/V_{vdw}$ value, (b) BPDA-DMDB with a large Δn and a large $\Delta\alpha/V_{vdw}$ value, and (c) 12FEDA-DCHM with a small Δn and a small $\Delta\alpha/V_{vdw}$ value. BPDA-ODA exhibits not only a large $\Delta\alpha/V_{vdw}$ value originating from BPDA moiety with a rigid structure and ODA with a polarizable ether oxygen,[33] but also a small Δn value due to the bent and flexible ether linkage. Such PIs that exhibit a large $\Delta\alpha/V_{vdw}$ and a small Δn value tend to have a smaller fraction of main chains oriented along the in-plane direction, concurrently with a larger fraction of main chains oriented along the out-of-plane direction (see Scheme 2a). This condition readily leads to an enhancement of $D_\perp$ in PI films. In such PIs, atomic vibrational energy transferring heat is effectively transmitted in the out-of-plane direction through the polymer chains. In contrast, BPDA-DMDB shows a small $D_\perp$ in spite of the large $\Delta\alpha/V_{vdw}$ value originating from the rigid BPDA and the rod-like DMDB structures. It can be assumed that the rigid-rod structure causes significant orientation of the main chains in the film plane during the spin-coating, drying, and curing processes. Such PIs having a large $\Delta\alpha/V_{vdw}$ and a large Δn value tend to exhibit small $D_\perp$ values as a result of the smaller fraction of the out-of-plane oriented main chains (see Scheme 2b). In such PIs, atomic vibrational energy is effectively transmitted in the in-plane direction of PI films, but not in the out-of-plane direction. Thereby, significant anisotropy in thermal diffusivity ($D_{||} - D_\perp$) should be observed. These PIs could be suitable for thermal conductive materials along the in-plane direction. However, BPDA-PDA, also having a large Δn and a large $\Delta\alpha/V_{vdw}$ value, exhibited a higher $D_\perp$ value (16.5×10^{-8} m^2/s) than that of BPDA-DMDB (10.3×10^{-8} m^2/s), the reason for which will be explained in the following section. In contrast, the small values of $\Delta\alpha/V_{vdw}$ and Δn observed for 12FEDA-DCHM originate from the highly flexible repeating unit owing to the multiple bent structures (−O− and −C(CF$_3$)$_2$−) and the bulky trifluoromethyl (−CF$_3$) side groups (see Scheme 2c). Such PIs with small $\Delta\alpha/V_{vdw}$ and small Δn values tend to exhibit small $D_\perp$ values due to the isotropic and homogeneous heat transfer within the film. Note that these phenomena suggest that a PI film containing a large fraction of the main chains oriented along the out-of-plane direction exhibits a large $D_\perp$ value. In other words, it is important to control the anisotropy in average phonon velocity to enhance the $D_\perp$ value of ~10-μm thick PI films. Meanwhile, the PI films derived from the diamines containing sulfur atoms in the main chain, i.e., BPDA-SDA, BPDA-DTDA, ODPA-SDA, and PMDA-DTDA (sulfur-containing PIs in Figure 1c), exhibit small $D_\perp$ values despite their small Δn and the relatively large $\Delta\alpha/V_{vdw}$ values; the reason will be explained in the following section.

Vuks Parameter $\Phi_\perp$ and Out-of-Plane Thermal Diffusivity. In the previous section, a tendency was found by which PI films having small Δn and large $\Delta\alpha/V_{vdw}$ values exhibit high $D_\perp$ values. In this section, a new parameter will be proposed which relates $D_\perp$ with the molecular structures of PIs representing the rigidity/linearity of repeating units, orientation of the main chains, and degree of molecular packing. As shown in Table 4, all PIs show positive polarizability anisotropy ($\Delta\alpha/V_{vdw} > 0$), which originates from the nearly linear molecular structures along the main chain (Z-axis) (see Scheme 1).

Table 4. Parameters Calculated for PI Model Structures Using the DFT Theory[a]

dianhydride	diamine	V_{vdw}	α_{zz}	α_{xx}	α_{yy}	$(\alpha_{xx} + \alpha_{yy})/2$	α_{av}/V_{vdw}	$\Delta\alpha/V_{vdw}$
BPDA	ODA	387.10	94.100	45.940	34.504	40.222	0.1503	0.1392
	TCDB	431.68	96.767	53.486	43.099	48.292	0.1493	0.1123
	DCDB	405.67	98.397	52.879	33.223	43.051	0.1516	0.1364
	PDA	306.62	72.273	38.316	25.366	31.841	0.1478	0.1319
	DCHM	432.11	86.015	48.237	36.995	42.616	0.1321	0.1004
	SDA	395.57	93.382	46.647	44.028	45.338	0.1551	0.1215
	BFAPOB	531.60	109.230	72.992	43.122	58.057	0.1413	0.0963
	DTDA	418.95	95.131	60.689	36.730	48.709	0.1532	0.1108
	TFDB	441.59	96.569	51.229	34.756	42.992	0.1378	0.1213
	DMDB	411.96	96.141	50.479	35.796	43.137	0.1476	0.1287
ODPA	ODA	393.14	91.026	41.794	41.146	41.470	0.1475	0.1261
	SDA	405.23	92.436	47.921	44.308	46.114	0.1519	0.1143
	BFAPOB	541.12	111.712	64.664	45.374	55.019	0.1366	0.1048
CBDA	ODA	298.42	53.512	33.827	28.865	31.346	0.1298	0.0743
6FDA	ODA	464.26	92.635	48.478	43.568	46.023	0.1326	0.1004
PMDA	DTDA	348.86	74.609	51.149	27.674	39.411	0.1466	0.1009
	ODA	312.89	69.467	41.514	24.188	32.851	0.1440	0.1170
P2FDA	ODA	322.30	69.304	41.982	24.273	33.128	0.1402	0.1122
	TCDB	369.54	74.232	46.817	33.493	40.155	0.1394	0.0922
	TFDB	375.91	72.789	40.685	30.086	35.385	0.1273	0.0995
12FEDA	DCHM	704.79	104.584	82.220	65.863	74.042	0.1195	0.0433

[a] The van der Waals volume (V_{vdw}), principal components of the polarizability tensor (α_{zz}, α_{xx}, α_{yy}), average polarizability in the direction normal to the PI main chain ($(\alpha_{xx} + \alpha_{yy})/2$), average polarizability per volume (α_{av}/V_{vdw}), and polarizability anisotropy per volume ($\Delta\alpha/V_{vdw}$).

Scheme 2. Optimized Structures of PI Repeating Units Obtained by DFT Calculations (above) and Schematic Illustration of the Ellipsoids of the Polarizability Tensor of the PI Repeating Units: (a)BPDA-ODA, (b)BPDA-DMDB, and (c)12FEDA-DCHM

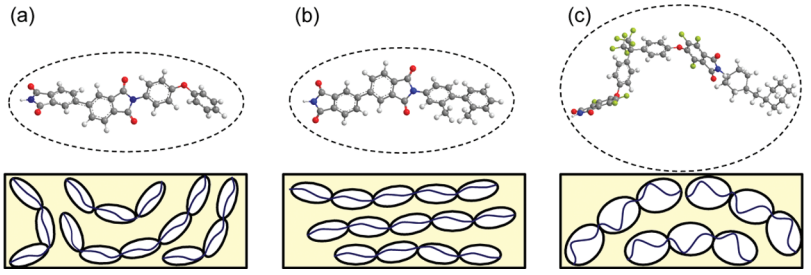

In addition, the nearly linear relationship with a positive slope in Figure 2a indicates that highly polarizable PIs with a large α_{av}/V_{vdw} value also accompany a large $\Delta\alpha/V_{vdw}$ value. Figures 2b and 2c show the relationships among α_{zz}/V_{vdw}, $(\alpha_{xx} + \alpha_{yy})/(2V_{vdw})$, and α_{av}/V_{vdw}. The range of variations for α_{zz}/V_{vdw} (0.1484−0.2441) is 4.2 times larger than that for $(\alpha_{xx} + \alpha_{yy})/(2V_{vdw})$ (0.0941−0.1171). The significant contribution of α_{zz}/V_{vdw} to α_{av}/V_{vdw} leads to the strong positive correlation between α_{av}/V_{vdw} and $\Delta\alpha/V_{vdw}$, as shown in Figure 2a. Meanwhile, the relationship between the average polarizabilities per volume (α_{av}/V_{vdw}) and the average refractive indices (n_{av}) is represented by eq 9. The Lorentz−Lorenz parameter, Φ_{av}, in eq 9 monotonously increases with an increase of α_{av}/V_{vdw} when K_p is constant. Accordingly, the Φ_{av} parameter, which can be readily estimated from the average refractive index (n_{av}), could increase with an increase of $\Delta\alpha/V_{vdw}$, which reflects the rigidity/linearity of the polymer repeating units. The Φ_{av} values estimated from the experimental n_{av} of the PIs are listed in Table 5, and the relationship between $D_\perp$ and Φ_{av} is depicted in Figure 3a. The Φ_{av} values reveal a weak and positive correlation with $D_\perp$, but the relationship is still unclear. This is because Φ_{av} only reflects the isotropic properties (average polarizability and molecular packing) without any information about the polymer chain orientation as represented by Δn; nonetheless $D_\perp$ is an apparently anisotropic property. Thus, based on the Vuks equation[23] which relates the polarizability anisotropy of polymers with the anisotropic refraction of light, we defined a new parameter, $\Phi_\perp$ designated as "Vuks parameter", as follows:

$$\Phi_\perp \equiv \frac{{n_\perp}^2 - 1}{{n_{av}}^2 + 2} = \frac{4\pi}{3} K_p \frac{\overline{\alpha}_\perp}{V_{vdw}} \tag{16}$$

Here $\overline{\alpha}_\perp$ in eq 16 is the macroscopic polarizability along the out-of-plane direction. The procedure to the estimate $\overline{\alpha}_\perp$ value for each PI film is as follows: (a) the packing coefficient, K_p, is estimated from the experimental n_{av} and the calculated α_{av}/V_{vdw} based on eq 9, (b) $\Phi_\perp$ is calculated using the experimental $n_\perp$ and n_{av}, and then (c) $\overline{\alpha}_\perp$ is estimated from the values of V_{vdw}, K_p, and $\Phi_\perp$ based on eq 16. It should be noted that parameter $\overline{\alpha}_\perp$, estimated from $\Phi_\perp$, reflects the macroscopic polarizability along the out-of-plane direction, whereas parameter α_{av}, calculated from the PI model structures, only reflects the microscopic polarizability of the repeating units. Thus, a PI film with a large fraction of out-of-plane oriented main chains (e.g., BPDA-ODA in Scheme 2a) should exhibit a large $\overline{\alpha}_\perp$ value. Using eqs 2 and 3 under the assumption that $(\Delta n)^2 \ll n_{av}$, eq 16 can be rewritten as

$$\Phi_\perp \equiv \frac{{n_\perp}^2 - 1}{{n_{av}}^2 + 2} = \Phi_{av} - \frac{4}{3}\frac{\Delta n}{{n_{av}}^2 + 2} \tag{17}$$

Figure 4a shows a contour plot of the calculated Vuks parameter $\Phi_\perp$ as a function of Δn and n_{av}. It is clearly shown that a decrease in Δn and an increase in n_{av} lead to an increase in $\Phi_\perp$, which coincides well with the fact that PI films having small Δn and large $\Delta\alpha/V_{vdw}$ values exhibited high $D_\perp$ values.

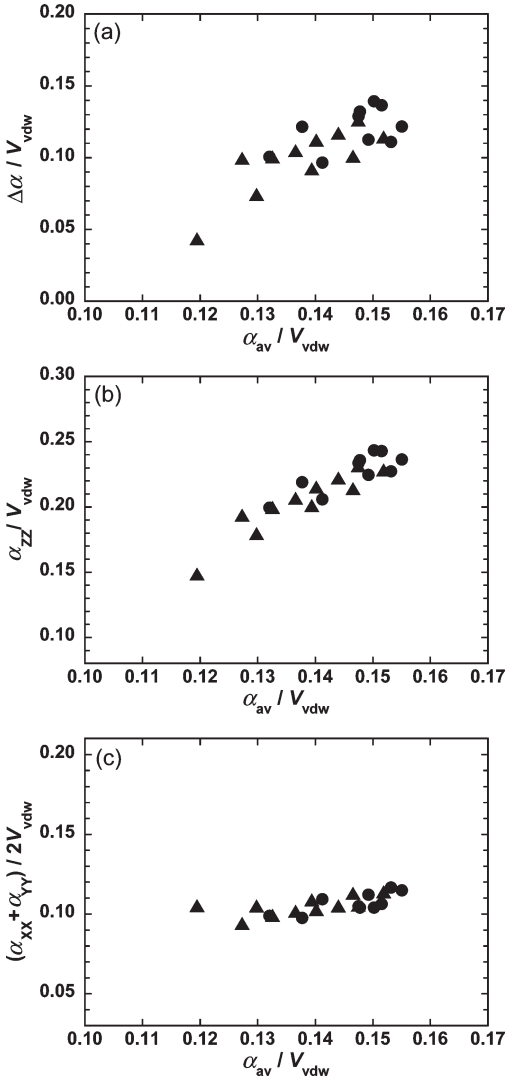

Figure 2. Relationships among polarizability anisotropy per volume ($\Delta\alpha/V_{vdw}$), average polarizability per volume (α_{av}/V_{vdw}), and principal components of polarizability tensors. (a) $\Delta\alpha/V_{vdw}$ versus α_{av}/V_{vdw}, (b) α_{zz}/V_{vdw} versus α_{av}/V_{vdw}, and (c) $(\alpha_{xx} + \alpha_{yy})/(2V_{vdw})$ versus α_{av}/V_{vdw} for the PIs derived from (●) BPDA dianhydride, and (▲) other dianhydrides.

To verify the validity of the Vuks parameter $\Phi_\perp$, the $\Phi_\perp$ values estimated from the experimental refractive indices (n_{av}, $n_\perp$) of the PI films are shown in Table 5, and the relationship between $D_\perp$ and $\Phi_\perp$ is plotted in Figure 3b. Note that the $\Phi_\perp$ values revealed an apparent positive correlation with $D_\perp$, except for the sulfur-containing PIs. From eq 17 and Figure 4a, it is clearly shown that PI films with small Δn and large n_{av} values exhibit high $\Phi_\perp$. The relationship between the experimental Δn and n_{av} values are shown in Figure 4b. Interestingly, this trend is similar to that of Figure 1c, which strongly suggests that the proposed parameter,$\Phi_\perp$, sensitively reflects the rigidity/linearity of the repeating units of the PIs and the orientation of main chains along the out-of-plane direction at the same time. As a consequence, the out-of-plane thermal diffusivity ($D_\perp$) of PI films can be estimated from the $\Phi_\perp$ value.

For the PIs derived from BPDA dianhydride, the $\Phi_\perp$ values decrease in the order of the diamine moiety: DTDA > SDA > ODA > TCDB > DCDB > PDA > DCHM > BFAPOB > TFDB > DMDB. This order is nearly the same as that of the $D_\perp$ values, except for the sulfur-containing PIs

Table 5. Lorentz−Lorenz Parameter (Φ_{av}), Vuks Parameter ($\Phi_\perp$), Molecular Packing Coefficient (K_p), and Out-of-Plane Polarizability per Volume ($\bar{\alpha}_\perp/V_{vdw}$) of PI Films (See Text)

dianhydride	diamine	Φ_{av}	$\Phi_\perp$	K_p	$\bar{\alpha}_\perp/V_{vdw}$
BPDA	ODA	0.3799	0.3669	0.6035	0.1451
	TCDB	0.3719	0.3604	0.5947	0.1447
	DCDB	0.3849	0.3567	0.6064	0.1404
	PDA	0.3993	0.3415	0.6457	0.1263
	DCHM	0.3468	0.3423	0.6267	0.1304
	SDA	0.3829	0.3738	0.5893	0.1514
	BFAPOB	0.3395	0.3366	0.5736	0.1401
	DTDA	0.3900	0.3862	0.6077	0.1517
	TFDB	0.3399	0.3187	0.5890	0.1292
	DMDB	0.3763	0.3155	0.6094	0.1236
ODPA	ODA	0.3638	0.3592	0.5888	0.1457
	SDA	0.3742	0.3738	0.5881	0.1517
	BFAPOB	0.3335	0.3302	0.5828	0.1352
CBDA	ODA	0.3392	0.3272	0.6240	0.1252
6FDA	ODA	0.3252	0.3206	0.5855	0.1307
PMDA	DTDA	0.3910	0.3762	0.6368	0.1410
	ODA	0.3744	0.3228	0.6213	0.1240
P2FDA	ODA	0.3604	0.3248	0.6140	0.1263
	TCDB	0.3565	0.3199	0.6109	0.1250
	TFDB	0.3266	0.2896	0.6128	0.1128
12FEDA	DCHM	0.3006	0.2987	0.6005	0.1187

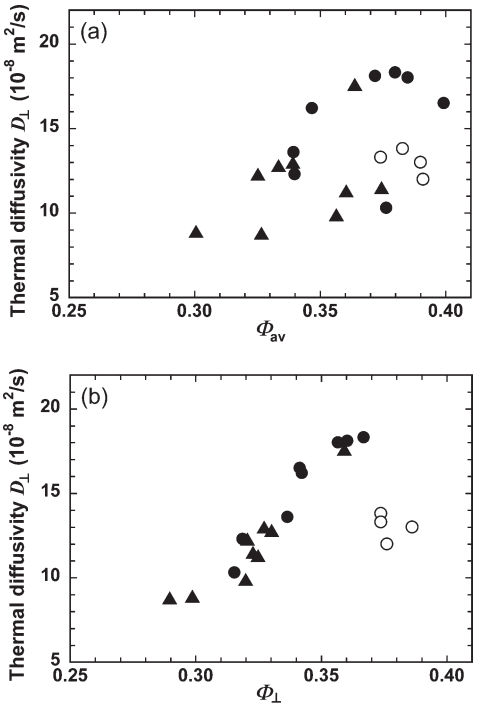

Figure 3. Out-of-plane thermal diffusivity ($D_\perp$) versus (a) Lorentz−Lorenz parameter Φ_{av}, and (b) Vuks parameter $\Phi_\perp$ calculated from the refractive indices for the PI films derived from (●) BPDA dianhydride, (▲) other dianhydrides, and (○) diamines containing sulfur atoms (sulfur-containing PIs).

(BPDA-DTDA and BPDA-SDA). On the other hand, the PIs derived from ODA diamine exhibit $\Phi_\perp$ values in a decreasing order with different dianhydride moieties: BPDA > ODPA > CBDA > P2FDA > PMDA > 6FDA. This order is also nearly the same as that of the $D_\perp$ values when compared to that of the Φ_{av} values. Meanwhile, as shown in Figure 3b, the sulfur-containing PIs, which include heavy sulfur atoms (atomic weight, A_r = 32.1) in the main chain, showed significantly smaller $D_\perp$ values than those expected from their $\Phi_\perp$. This phenomenon can be explained by the reduced average phonon velocity along the polymer chains due to the heavy atom effect. As seen in eq 1, thermal diffusivity D is

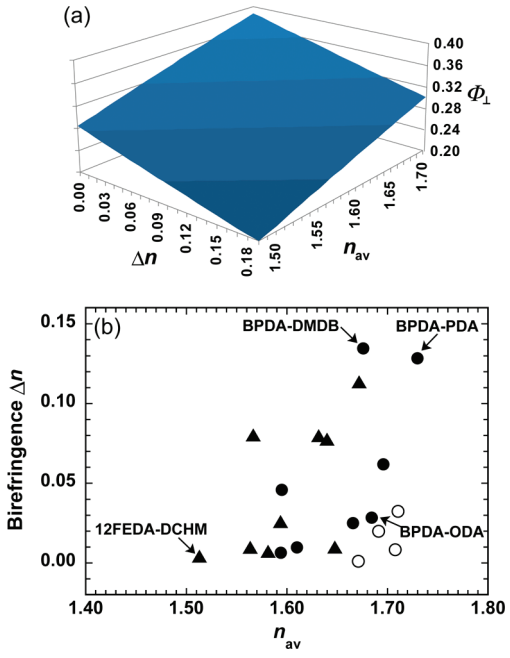

Figure 4. Relationships among refractive indices (n_{av}), birefringences (Δn), and Vuks parameter $\Phi_\perp$ values of PI films. (a) Contour plot of $\Phi_\perp$ as a function of n_{av} and Δn. (b) Δn versus n_{av} for the PIs derived from (●) BPDA dianhydride, (▲) other dianhydrides, and (○) diamines containing sulfur atoms (sulfur-containing PIs).

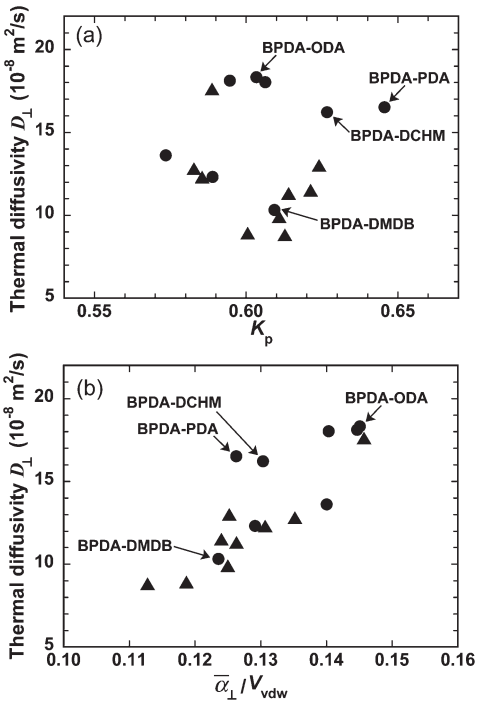

Figure 5. Relationships among out-of-plane thermal diffusivity ($D_\perp$), molecular packing coefficient (K_p), and out-of-plane polarizability per volume ($\bar{\alpha}_\perp/V_{vdw}$). (a) $D_\perp$ versus K_p, and (b) $D_\perp$ versus $\bar{\alpha}_\perp/V_{vdw}$ for the PIs derived from (●) BPDA dianhydride, and (▲) other dianhydrides.

the product of average phonon velocity (v) and the mean free path of phonons (l). Since v is proportional to $(f/M)^{1/2}$, where M is the mass of the oscillators and f is the force constant between couplings,[7] sulfur-containing moieties having higher M in the PI chains considerably lower v, which readily lowers the $D_\perp$ values. Moreover, the large difference in atomic weight between sulfur and neighboring carbons (A_r = 12.0) in sulfur-containing PIs than those among carbon, oxygen (16.0), and nitrogen (14.0) atoms in sulfur-free PIs should cause significant phonon scattering. It is well-known that the $(f/M)^{1/2}$ term is also proportional to the frequency of infrared (IR) absorption. As an example, the stretching vibration at the C−O−C bond in diphenyl ether (Ph−O−Ph) is observed at 1237 cm^{-1}, whereas those at the C−S−C bonds in diphenyl thioether (Ph−S−Ph) and diphenyl sulfone (Ph−SO_2−Ph) are observed at 689 cm^{-1} and 730/592 cm^{-1}, respectively.[34] The much smaller wavenumbers in the latter also support the reduced phonon velocity in the sulfur-containing PIs.

Moreover, to get more detailed insight into the molecular structures of PI films with $D_\perp$, the contributions of K_p and $\bar{\alpha}_\perp/V_{vdw}$ to $\Phi_\perp$ were evaluated using eq 16. Note that parts a and b of Figure 5 show the K_p and the $\bar{\alpha}_\perp/V_{vdw}$ dependences on $D_\perp$ except for sulfur-containing PIs, respectively. A nonlinear but positive correlation is seen between $\bar{\alpha}_\perp/V_{vdw}$ and $D_\perp$, whereas the relation between $D_\perp$ and K_p is unclear. The positive correlation between $\bar{\alpha}_\perp/V_{vdw}$ and $D_\perp$ suggests that a PI film containing a large fraction of out-of-plane oriented main chains shows a large $D_\perp$ value, which agrees with the tendency described in the previous section. For the PIs derived from BPDA dianhydride, the $\bar{\alpha}_\perp/V_{vdw}$ values decrease in the order of the diamine moiety: ODA > TCDB > DCDB > BFAPOB > DCHM > TFDB > PDA > DMDB. Compared with the order of $D_\perp$, BPDA-DCHM and BPDA-PDA exhibit larger $D_\perp$ values than those expected from their $\bar{\alpha}_\perp/V_{vdw}$. This could be caused by the larger K_p, which represents the dense molecular packing than the other PIs (see Figure 5a). Scheme 3 shows the optimized geometries of

Scheme 3. Optimized Structures of PI Repeating Units Obtained by DFT Calculations (above) and Schematic Illustration of the Ellipsoids of Polarizability Tensor of the PI Repeating Units: (a) BPDA-DCHM; (b) BPDA-PDA

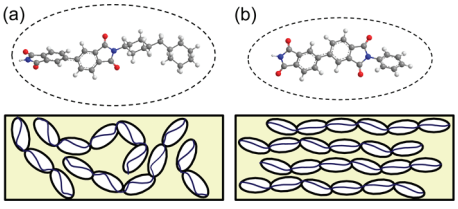

the repeating units and their schematic illustrations of polarizability tensors for BPDA-DCHM and BPDA-PDA PIs. The molecular rigidity of the former is not as high as that of the latter, which is due to the bent and bulky structure in the DCHM moiety. However, the isotropic orientation of the PI chains, as evaluated from grazing incidence wide-angle X-ray scattering,[35] and the relatively high K_p value (0.6244) of BPDA-DCHM could enhance the $D_\perp$ value (16.2×10^{-8} m^2/s). In contrast, although the main chains are preferentially aligned in the film plane the same as BPDA-DMDB (see Scheme 2b), BPDA-PDA (see Scheme 3b) exhibits a high $D_\perp$ value (16.5×10^{-8} m^2/s). For the semicrystalline BPDA-PDA, the main chains are highly ordered through the face-to-face stacking of imide and phenyl planar groups,[36,37] which is reflected in the largest K_p value (0.6358) in the PIs of this study. In contrast, the K_p of BPDA-DMDB (0.6082) is not so high, owing to the bulky −CH_3 groups in DMDB, which cause loose chain packing. Accordingly, BPDA-DMDB exhibits the smallest $D_\perp$ value (10.3×10^{-8} m^2/s). This is why the PIs with bulky side chains (−CH_3 and −CF_3) exhibit relatively small $D_\perp$ values. These results clearly indicate that the $D_\perp$ of PI films is significantly influenced, not only by the main chain orientations and the rigidity/linearity of the polymer structure,

Table 6. Out-of-Plane Thermal Diffusivities ($D_\perp$), In-Plane Refractive Indices ($n_{||}$), Out-of-Plane Refractive Indices ($n_\perp$), Average Refractive Indices (n_{av}), In-Plane/Out-of-Plane Birefringences (Δn), and $\Phi_\perp$ Value of Amorphous Polymer Films[b]

amorphous polymer[a]	thermal diffusivity $D_\perp$($\times 10^{-8}$ m^2/s)	$n_{||}$	$n_\perp$	n_{av}	Δn	$\Phi_\perp$	ref.
PET	6.2	1.6506	1.5033	1.6015	0.1473	0.2760	39, 41
PMMA	10.8	1.4869	1.4869	1.4869	0.0000	0.2876	38, 40
PS	11.5	1.5844	1.5852	1.5847	−0.0008	0.3354	38, 40
PES	14.2	1.6395	1.6331	1.6373	0.0064	0.3561	38
PC	17.3	−	−	1.5875	0.0001	0.3363	38, 42, 43

[a] PET, polyethyleneterephthalate; PMMA, poly(methyl methacrylate); PS, polystyrene; PES, poly(ether sulfone); PC, polycarbonate. [b] The values of $D_\perp$ and refractive indices are taken from refs 38−43.

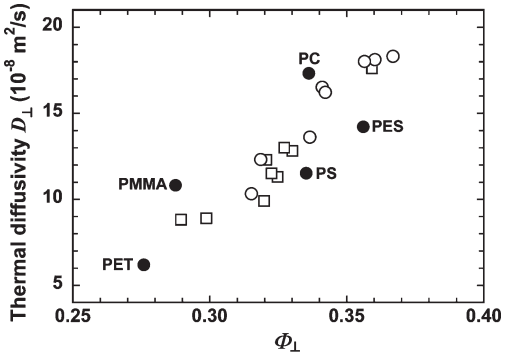

Figure 6. Out-of-plane thermal diffusivity ($D_\perp$) versus Vuks parameter $\Phi_\perp$ for films of (●) typical amorphous polymers, PIs derived from (○) BPDA dianhydride and (□) other dianhydrides. The $\Phi_\perp$ values were estimated from their refractive indices.

but also by the degree of molecular packing. It also suggests that the intermolecular van der Waals interactions cannot be ignored in the out-of-plane thermal diffusivity of amorphous polymer films because of the small absolute values of $D_\perp$ compared to $D_{||}$.

In summary, we proposed a new parameter, $\Phi_\perp$, based on modified Vuks equations, which can be used to assess the anisotropic thermal diffusivity of PI films in the out-of-plane direction ($D_\perp$). The Vuks parameter $\Phi_\perp$ can be readily estimated from the experimental refractive indices, and it connects the $D_\perp$ values with the molecular structures of PIs. The $D_\perp$ of the PIs having rod-like structures significantly depends on the rigidity/linearity of the molecular structure and the orientation of the main chains. Furthermore, the estimation of the contributions of K_p and $\overline{\alpha}_\perp/V_{vdw}$ to $\Phi_\perp$ clarified that the $D_\perp$ of the PIs are essentially determined by the magnitude of $\overline{\alpha}_\perp/V_{vdw}$ (the macroscopic out-of-plane polarizability in the films). For instance, the $\overline{\alpha}_\perp/V_{vdw}$ values can be defined not only for the polymers with positive birefringence like PIs, but also for other amorphous polymers having negative birefringence. Table 6 shows the relationship between $D_\perp$ and $\Phi_\perp$ of five kinds of typical amorphous polymers, polyethyleneterephthalate (PET), poly(methyl methacrylate) (PMMA), polystyrene (PS), poly(ether sulfone) (PES), and polycarbonate (PC). The $D_\perp$ values were measured by the TWA method for PS,[38] PMMA,[38] PES,[38] PC,[38] and by the photoacoustic method for PET.[39] The refractive indices ($n_{||}$, $n_\perp$, and n_{av}), which have been measured using a prism coupler at a wavelength of 633 nm were used to calculate $\Phi_\perp$ values of PS,[40] PMMA,[40] and PET,[41] while the refractive indices of PES were measured in this study due to the lack of reference. In the case of PC, the values of n_{av} and Δn were measured using an Abbe refractometer,[42] and a Zeiss polarizing microscope, and an Ehringhaus calcite-plate rotary compensator,[43] respectively. Although different film samples were used for the measurements of $D_\perp$ and the refractive indices, the $\Phi_\perp$ values reported in the references also revealed a positive correlation with $D_\perp$ (see Table 6 and Figure 6). The PES film, which includes sulfur atoms with a sulfonyl group in the main chain, showed a lower $D_\perp$ than that predicted from its $\Phi_\perp$; it is explainable by the heavy sulfur atom effect, as seen in the sulfur-containing PIs. Hence, we consider that the proposed Vuks parameter, $\Phi_\perp$, is applicable as a measure of $D_\perp$, not only to relatively rigid aromatic polymers like PIs, but also to other amorphous polymers.

Conclusion

The dependence of the thermal diffusivity along the out-of-plane direction ($D_\perp$) on molecular structure, chain orientation, and molecular packing was extensively investigated for 21 kinds of spin-coated aromatic and semiaromatic polyimide (PI) films using temperature wave analysis. The degree of chain orientation as represented by Δn and P_{200}, the rigidity/linearity of polymer repeating units as represented by $\Delta\alpha/V_{vdw}$, and the degree of molecular packing as represented by K_p were quantitatively evaluated by the experimental refractive indices and the calculated polarizability tensors of the repeating units of the PIs. PIs having linear and rigid molecular structures with lower degrees of molecular orientation of the main chains along the in-plane direction exhibited higher values of $D_\perp$. This phenomenon could be explained by the directional dependence of average phonon velocity. In PI films, thermal energy is transferred more efficiently through covalent bonds and aromatic rings along the polymer chains than among polymer chains which weakly interact through van der Waals interactions. Thus, BPDA-ODA, which has a lower degree of in-plane orientation owing to the bent ether linkage at the diamine moiety with maintaining the rigid/linear repeating unit due to the dianhydride moiety, showed the highest $D_\perp$ value in this study. Such PI films with high thermal conductivity are promising for interlayer insulators or buffer coatings in microelectronics and optoelectronics devices with large power consumption.

In order to correlate the molecular structure, chain orientation, and molecular packing of PI films with their thermal diffusivity along the out-of-plane direction, $D_\perp$, we proposed a new parameter, $\Phi_\perp$, based on modified Vuks equations, which can be used to estimate $D_\perp$, and the validity of the parameter was examined. The Vuks parameter $\Phi_\perp$ is easily calculated from the experimental refractive indices and it could explain the complicated behavior of $D_\perp$, not only by the rigidity/linearity of the molecular structure and the orientation of the main chains, but also by the degree of molecular packing. In addition, $\Phi_\perp$ values estimated from the references revealed a positive correlation with $D_\perp$ in typical amorphous polymer films. We consider that the Vuks parameter $\Phi_\perp$ can be used as a key measure for predicting the thermal conductivity of amorphous polymers.

Acknowledgment. The authors thank Mizuka Tanimoto and Hong Gao at the Tokyo Institute of Technology for discussions with valuable suggestions, and for synthesizing the PIs using BFAPOB diamine. We also acknowledge Toshimasa Hashimoto and Junko Morikawa at the Tokyo Institute of Technology for valuable advice on the TWA method, and for offering typical amorphous polymer samples.

Supporting Information Available: Figure showing the relationships among the orientation function (P_{200}), polarizability anisotropy per volume ($\Delta\alpha/V_{vdw}$), and thermal diffusivity ($D_{\perp}$) of PI films. This material is available free of charge via the Internet at http://pubs.acs.org.

Note Added after ASAP Publication. This article posted ASAP on August 16, 2010. Equation 1 and the sentence following the equation have been revised. The correct version posted on August 24, 2010.

References and Notes

(1) Cha, H. J.; Hedrick, J.; Dipietro, R. A.; Blume, T.; Beyers, R.; Yoon, D. Y. *Appl. Phys. Lett.* **1996**, *68*, 1930–1932.
(2) Burrows, P. E.; Gu, F.; Bulovic, V.; Shen, Z.; Forrest, S. R.; Thompson, M. E. *IEEE Trans. Electron Devices* **1997**, *44*, 1188–1203.
(3) Choy, C. L. *Polymer* **2001**, *18*, 984–1004.
(4) Kurabayashi, K. *Int. J. Thermophys.* **2001**, *22*, 277–288.
(5) Pietralla, M.; Weeger, R. M.; Mergenthaler, D. B. *Z. Phys. B, Condensed Matter* **1989**, *77*, 219–228.
(6) Choy, C. L.; Luk, W. H.; Chen, F. C. *Polymer* **1978**, *19*, 155–162.
(7) Pietralla, M. *J. Comput. Aided Mater. Des.* **1996**, *3*, 273–280.
(8) Venerous, D. C.; Kolev, D. N. *Macromolecules* **2009**, *42*, 2594–2598.
(9) Broerman, A. W.; Venerous, D. C.; Schieber, J. D. *J. Chem. Phys.* **1999**, *111*, 6965–6969.
(10) Shonaike, G. O.; Advani, S. G. *Advanced Polymer Materials*; CRC Press: New York, 2003.
(11) Kurabayashi, K.; Goodson, K. E. *J. Appl. Phys.* **1999**, *86*, 1925–1931.
(12) Takahashi, F.; Ito, K.; Morikawa, J.; Hahimoto, T.; Hatta, I. *Jpn. J. Appl. Phys.* **2004**, *43*, 7200–7204.
(13) Morikawa, J.; Hashimoto, T. *J. Appl. Phys.* **2009**, *105*, 113506.
(14) Terui, Y.; Ando, S. *J. Polym. Sci., Part B* **2004**, *42*, 2354–2366.
(15) Hashimoto, T.; Morikawa, J.; Kurihara, T.; Tsuji, T. *Thermochim. Acta* **1997**, *304/305*, 151–156.
(16) Tagaya, A.; Iwata, S.; Kawanami, E.; Tsukahara, H.; Koike, Y. *Jpn. J. Appl. Phys* **2001**, *40*, 6117–6123.
(17) Henning, J. *J. Polym. Sci. C* **1967**, *16*, 2751–2762.
(18) Matsuda, S.; Ando, S. *J. Polym. Sci. B* **2003**, *41*, 418–428.
(19) Hatori, H.; Yamada, Y.; Shiraishi, M. *Carbon* **1993**, *31*, 1307–1312.
(20) Jarvis, D. A.; Hutchinson, I. J.; Bower, D. I.; Ward, I. M. *Polymer* **1980**, *21*, 41–54.
(21) Lorentz, H. A. *Ann. Phys. Chem.* **1880**, *11*, 641–665.
(22) Lorenz, L. *Ann. Phys. Chem.* **1880**, *11*, 70–103.
(23) Vuks, M. F. *Opt. Spectrosc.* **1964**, *20*, 361–364.
(24) Qiu, Z.; Wang, J.; Zhang, Q.; Zhang, S.; Ding, M.; Gao, L. *Polymer* **2006**, *47*, 8444–8452.
(25) Matsumoto, T. *High Perform. Polym.* **1999**, *11*, 367–377.
(26) Oishi, Y.; Ogasawara, K.; Hihara, H.; Mori, K. *J. Photopolym. Sci. Technol.* **2001**, *14*, 37–40.
(27) Lee, C.; Yang, W.; Parr, R. G. *Phys. Rev. B.* **1988**, *37*, 785–789.
(28) Miehlich, B.; Savin, A.; Stoll, H.; Preuss, H. *Chem. Phys. Lett.* **1989**, *157*, 200–206.
(29) Becke, A. D. *J. Chem. Phys.* **1993**, *98*, 5648–5652.
(30) Frisch, M. J.; Trucks, G. W.; Schlegel, H. B.; Scuseria, G. E.; Robb, M. A.; Cheeseman, J. R.; Montgomery, J. A., Jr.; Vreven, T.; Kudin, K. N.; Burant, J. C.; Millam, J. M.; Iyengar, S. S.; Tomasi, J.; Barone, V.; Mennucci, B.; Cossi, M.; Scalmani, G.; Rega, N.; Petersson, G. A.; Nakatsuji, H.; Hada, M.; Ehara, M.; Toyota, K.; Fukuda, R.; Hasegawa, J.; Ishida, M.; Nakajima, T.; Honda, Y.; Kitao, O.; Nakai, H.; Klene, M.; Li, X.; Knox, J. E.; Hratchian, H. P.; Cross, J. B.; Bakken, V.; Adamo, C.; Jaramillo, J.; Gomperts, R.; Stratmann, R. E.; Yazyev, O.; Austin, A. J.; Cammi, R.; Pomelli, C.; Ochterski, J. W.; Ayala, P. Y.; Morokuma, K.; Voth, G. A.; Salvador, P.; Dannenberg, J. J.; Zakrzewski, V. G.; Dapprich, S.; Daniels, A. D.; Strain, M. C.; Farkas, O.; Malick, D. K.; Rabuck, A. D.; Raghavachari, K.; Foresman, J. B.; Ortiz, J. V.; Cui, Q.; Baboul, A. G.; Clifford, S.; Cioslowski, J.; Stefanov, B. B.; Liu, G.; Liashenko, A.; Piskorz, P.; Komaromi, I.; Martin, R. L.; Fox, D. J.; Keith, T.; Al-Laham, M. A.; Peng, C. Y.; Nanayakkara, A.; Challacombe, M.; Gill, P. M. W.; Johnson, B.; Chen, W.; Wong, M. W.; Gonzalez, C.; Pople, J. A. *Gaussian 03, Revision E.01*, Gaussian, Inc.: Wallingford CT, 2004.
(31) Slonimskii, G.; Askadskii, A.; Kitaigodorodskii, A. *Polym. Sci. U.S.S.R* **1970**, *12*, 556–577.
(32) Bondi, A. *J. Phys. Chem.* **1964**, *68*, 441–451.
(33) Miller, K. J. *J. Am. Chem. Soc.* **2006**, *112*, 8533–8542.
(34) SDBSWeb: http://riodb01.ibase.aist.go.jp/sdbs/ (National Institute of Advanced Industrial Science and Technology, 17/04/2010).
(35) Wakita, J.; Jin, S.; Shin, T. J.; Ree, M.; Ando, S. *Macromolecules* **2010**, *43*, 1930–1941.
(36) Ree, M.; Kim, K.; Woo, S. H.; Chang, H. *J. Appl. Phys.* **1997**, *81*, 698–708.
(37) Toney, M. F.; Russell, T. P.; Logan, J. A.; Kikuchi, H.; Sands, J. M.; Kumar, S. K. *Nature* **1995**, *374*, 709–711.
(38) Morikawa, J.; Tan, J.; Hashimoto, T. *Polymer* **1995**, *36*, 4439–4443.
(39) Korpiun, P.; Merte, B.; Fritsch, G.; Tilgner, R.; Luscher, E. *Colloid Polym. Sci.* **1983**, *261*, 312–318.
(40) Agan, S.; Ay, F.; Kocabas, A.; Aydinli, A. *Appl. Phys. A: Mater. Sci. Process.* **2005**, *80*, 341–345.
(41) Bai, S. J.; Spry, R. J.; Zelmon, D. E.; Ramabadran, U.; Jackson, J. *J. Polym. Sci., Part B* **1992**, *30*, 1507–1514.
(42) Uchiyama, A.; Ikeda, Y.; Yatabe, T. *Kobunshi Ronbunshu* **2003**, *60*, 38–44.
(43) Wu, M. S. *J. Appl. Polym. Sci.* **1986**, *32*, 3263–3275.